논문 97-8-1-09

고전압 실험실에서 시변성 전자계의 특성

Characteristics of Time-Changing Electric and Magnetic Fields at a High Voltage Laboratory

이복희 · 이경옥 · 안창환

Bok-Hee Lee · Kyoung-Ok Lee · Chang-Hwan Ahn*

요 약

본 논문은 고전압 실험실에서 시변성 전자계의 측정 및 평가에 관한 것으로 전자적 외란은 주로 전력장비의 지락고장 및 개폐조작에 의해 기인되며, 전자회로와 제어장비들은 전자방해작용에 매우 민감하다. 주어진 전자환경에 대한 전자방해작용의 레벨을 평가하는 것은 필수적이다. 전계는 40 Hz~200 MHz 범위의 대역폭을 갖는 전계센서로 관측되었으며, 시변성 자계는 출력이 입사신호에 직접적으로 비례하는 루프형 센서로 측정되었다. 또한 진동성 과도전류와 차단파 임펄스전압에 의해 유도된 전자방해작용의 레벨과 전자 차폐의 외함설계에 관한 정보를 주는 시변성 전자계의 주파수 성분을 고속프리에변환으로 분석하였다.

Abstract

This paper deals with measurements and evaluation of the time-changing electric and magnetic fields at a high-voltage laboratory. The electromagnetic disturbances originate mainly from ground faults and on/off operations of electric power equipments. The electronic circuits and control devices are very sensitive to electromagnetic interferences. It is necessory to evaluate the levels of interferences for a given electromagnetic environment. The electric field was observed by the electric field sensor having the bandwidth of the range from 40 Hz to 200 MHz, and the time-changing magnetic field was measured by the loop sensor of which the output is directly proportional to the incident signal. Also, the frequency components of the time-changing electric and magnetic fields induced by an oscillatory transient current and a chopped impulse voltage were analyzed by terms of the fast Fourier transformation, and those give the information about the levels of the electromagnetic interferences and the design of the electromagnetic shielding enclosures.

I. Introduction

Influences of electromagnetic fields have discussed with the development of digital instruments during the recent years. The undesirable radiation of electromagnetic energy into the surrounding space originate from the time-changing electric and magnetic fields due to the switching operations of electric power

인하대학교 전기공학과(Dept. of Electrical Engineering, Inha University)
· 논문번호 : 961231-071
· 접수일자 : 1996년 12월 31일

equipments. Large amounts of such energy inevitably leak into the space around the electronic equipments, and those are conducted over control power lines to other devices. The conducted and/or radiated electromagnetic energy acts as injurious interferences to telecommunication control device and is capable of causing the serious failures in electric power systems as well as possibility of biological hazards[1]~[3]. The electronic control devices are generally exposed to the electric, the magnetic and the electromagnetic fields.

The small-sized electronic circuits, whether they use discrete components or integrated circuits, are susceptible to malfunction or damage caused by transient electromagnetic interferences. The transient electromagnetic interferences such as lightning, electromagnetic pulse(EMP), and switching surges commonly have peak voltages and currents that are significantly larger than the tolerance of electronic circuits. The electromagnetic interferences from electric power transmission lines are to affect the amplitude modulated communication services such as radio and television. A number of measurements and calculation methods of transient electromagnetic fields were developed for EMP applications[4],[5].

The analysis of the electric and magnetic fields components by means of the Fourier spectrum is of primary importance because the evaluation for non-repetitive pulses is very suitable in the wide frequency range. The electromagnetic shielding was employed because the effective protection of the electronic instruments and control devices is directly associated with the frequency of magnetic field components.

In order to prevent the effect of electromagnetic disturbances on the computer-controlled equipments and electronic circuits, the study of electromagnetic field measuring techniques is important. In this work, for the purpose of evaluating the transient electric and magnetic fields in the vicinity of high voltage test equipments, the new electric and magnetic field measuring devices have been designed and fabricated, and the actual surveys have been carried out.

The present paper contributes to the measurement results of the time changing electric and magnetic fields induced by an oscillatory transient current simulator and by a chopped impulse voltage at a high voltage laboratory. The measured data were analyzed by the fast Fourier transformation(FFT) method.

Ⅱ. Measuring Devices and Experimental Procedures

The electric field(E-field) measuring device structure is very simple as shown in Fig. 1. In reality, since the electric field signal of steep fronted surges or microwaves gets in the live electrode of the E-field sensor, the input signal has to be transmitted to the data recorder with the distortion free. The capacitance C_1 is the parasitic capacitance between the powered live conductor and the sensing electrode of the E-field sensor, whereas the capacitance C_2 is the capacitance of the E-field sensor, which is formed by a thin film layer of the insulating medium (polypropylene, thickness: 22 μm, relative permittivity: 2.16) inserted between the opposite flat surface of live electrode and the earthed electrode.

The characteristic impedance must be matched from the live electrode of the E-field sensor to the data recorder. In order to match the characteristic impedance, the E-field sensor was designed with a conical type. For conical geometry, the characteristic impedance Z_0 is expressed as [6] :

$$Z_0 = \frac{138}{\sqrt{\varepsilon_s}} \log_{10} \frac{r_2}{r_1} \ [\Omega] \qquad (1)$$

where r_1 is the outside radius of inner conductor, r_2 is the inside radius of outer conductor and ε_s is the relative permittivity of filling gas.

If the ratio of r_1 to r_2 at the conical part of the E-field sensor is given, the characteristic impedance can be determined. Thus, to obtain the characteristic impedance of 50 Ω, the E-field sensor was designed so that r_2/r_1 is equal to 2.302 at the conical part.

The principal characterizations are constituted of the step response and intrinsic parameters of the E-field sensor. In order to evaluate the step response characteristics of the E-field sensor, a special transmission arrangement was used. The rising time of the E-field sensor is about 1.75 ns. The high cutoff frequency is calculated from the transfer function and then is about 200 MHz[7].

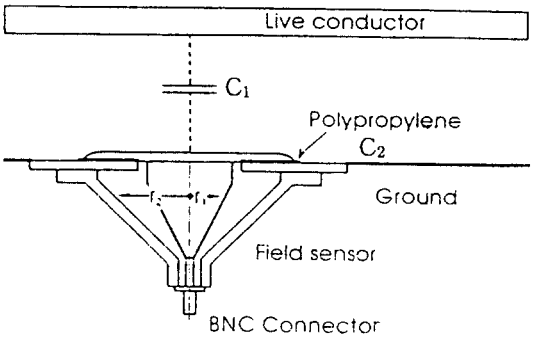

Fig. 1. Schematic diagram of the E-field sensor.

The attenuation on the tail of step response is to be attributed to the E-field sensor capacitance C_2 and the input impedance R of oscilloscope. Also the low cutoff frequency of the E-field sensor calculated from the decay time constant of step response is about 40 Hz with oscilloscope-input impedance of 1 MΩ. Therefore, the frequency bandwidth of the electric field measuring device is a range from 40 Hz to 200 MHz and its sensitivity is about 60.6 mV/kV/m.

On the other hand, the measuring sensor of the time-changing magnetic field has a loop structure with the signal transmission cables. The magnetic field (B-field) sensor is required the electrostatic shield to reduce the electric field from coupling into the sensor.

The B-field sensor, which is the self-integrated loop type, was made of coaxial cable so as to minimize the effect of external electric field disturbances. The outer conductor of the coaxial cable is snapped and the integrated resistor is connected across the gap, and the center conductor of the coaxial cable is terminated at the outer conductor as shown in Fig. 2. The output of the B-field sensor is proportional to the applied magnetic field for time domain data[8].

The radius of the B-field sensor is 60 mm and the self-integrated resistance is 50 Ω. Calibration experiments which enable to the accurate response determination of the B-field measuring system by unit step input were carried out. The sensitivity of the B-field measuring system was determined by using an

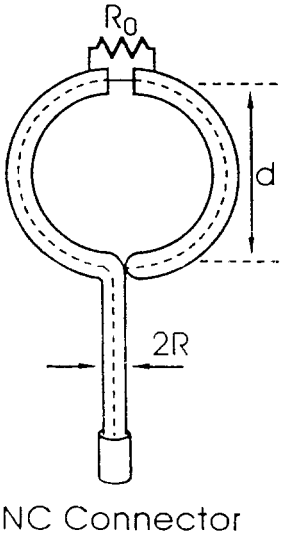

Fig. 2. Self-integrated loop sensor for measuring a time-changing magnetic field.

auxiliary coil recommended by ANSI/IEEE Std 644[9]. A measurement of the current flowing into the auxiliary coil was made by the CT1(Tek.) current probe. The sensitivity of the B-field measuring system was investigated on the basis of the geometry of the B-field sensor, and then the sensitivity is about 40 mV/μT. The frequency bandwidth of the B-field measuring system ranges from 700 kHz to 120 MHz.

The optical link was used to reduce the effect of the measured electric and magnetic fields. All the output signals were recorded by a digitizer having a bandwidth of 350 MHz and were analyzed by FFT technique.

The oscillatory transient current simulator was fabricated by a series R-L-C loop as shown in Fig. 3, and the circuit simulates the ground faults and/or the short circuit from the practical electric power equipments. No inductor was separately connected at the simulator be-

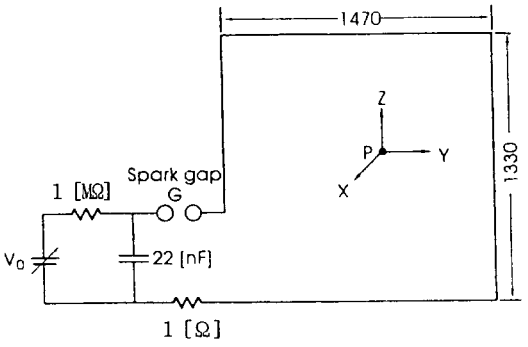

Fig. 3. Circuit diagram for a simulator of the oscillatory transient current.

cause there always exist parasitic series inductances in the short circuit.

Fig. 4 shows the measuring arrangement for the chopped impulse experiments in a high voltage laboratory. The metal screen fence was made of the copper mesh of 1.5×1.5 mm².

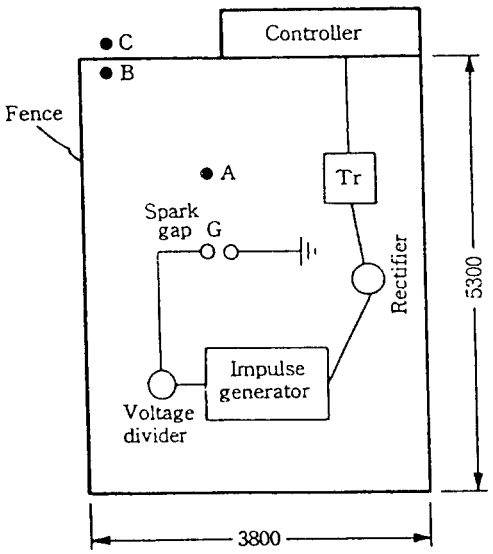

Fig. 4. Layout of the high voltage laboratory with the position of the measuring points and equipments.

The electric and magnetic fields, which are induced by the air discharges of sphere to sphere gap biased with the impulse voltage, have been measured at a high voltage laboratory. Owing to the careful shielding of the digitizer and the optical link, the precise data could be observed.

Ⅲ. Results and Discussion

3-1 Electric and magnetic fields from simulator

The output of a digitizer used during the experiments is a time-domain waveform, but the resonance frequency of the measured response can be determined by the FFT processing. Fig. 5 shows a typical waveform of the oscillatory transient currents and its FFT result, and the charging voltage V_0 at that time was 2.5 kV in Fig. 3.

The maximum current approximately depends on the charging voltage V_0 and the inductance L of the short circuit loop. The oscillatory transient current is obviously superimposed on two frequencies and their resonance points are remarked as two peaks in the FFT result. The oscillatory transient current begins with a high oscillatory frequency and is continued into a low damped oscillatory frequency of 390 kHz, which is determined by the circuit constants of the R-L-C loop.

The frequency component of about 20 MHz, which is located at the wavefront and in the vicinity of peak values, may be due to the discharge characteristic of the spark gap G and the charge and discharge characteristics of the capacitor charged to a voltage V_0.

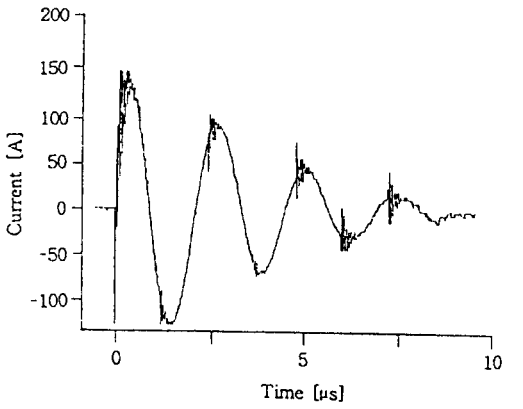

(a) Trancient oscillatory current waveform.

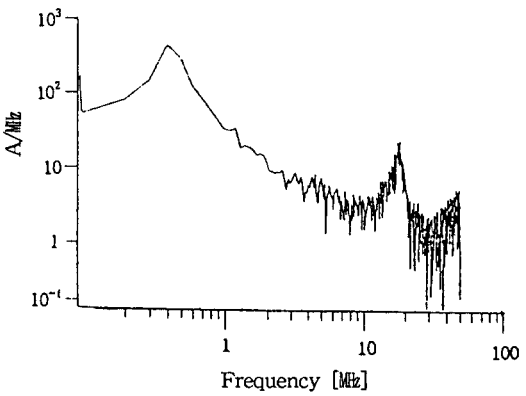

(b) FFT.

Fig. 5. The oscillatory transient current waveform and its FFT result.

In order to evaluate the radiation coupling characteristic between the time-changing electric and magnetic fields, E_y and B_x components were measured at the point of P in Fig. 3.

Then the E-field sensor indicates the average intensity of the electric field detected by the sensor in a non-uniform field. Fig. 6 shows the typical waveforms of the electric and magnetic fields and their FFT results. Where dB kV/m/MHz is the decibel above 1 kV/m/

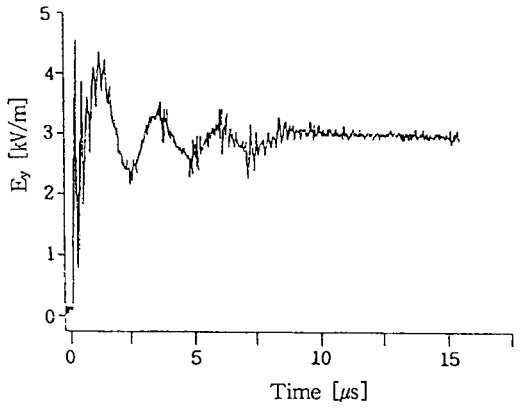

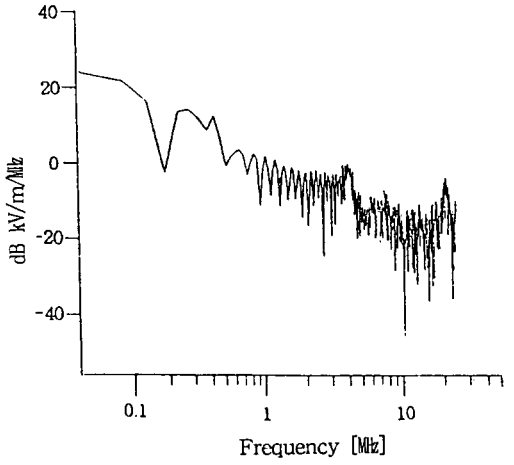

(a) Typical waveform of the electric field E_y and its FFT.

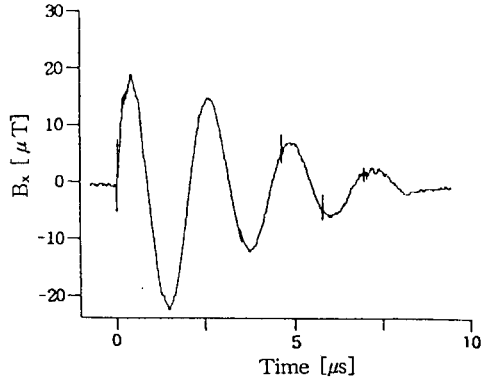

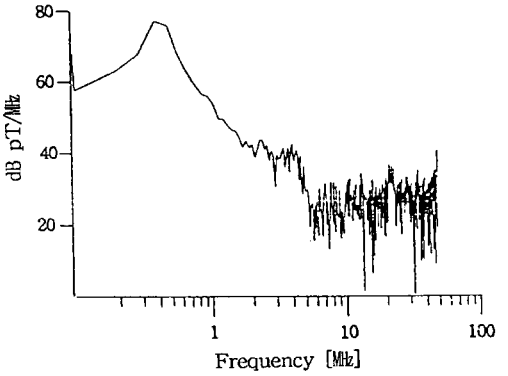

(b) Typical waveform of the magnetic flux density B_x and its FFT.

Fig. 6. Waveforms of the electric and magnetic fields at the point P and their FFT results.

MHz and dB pT/MHz is the decibel above 1 pT/MHz, respectively.

The B-field loop sensor detects the time derivative of the applied magnetic field, but the self-integrated resistance converts the sensing signal to an output signal proportional to the applied magnetic field. The output of the B-field sensor indicates the actual magnetic field within the frequency bandwidth of measuring system. Therefore, the measured magnetic flux density waveform is principally similar to the reference current waveform. However, the amplitude of the frequency component of less than 390 kHz may be attenuated by the limit of low cut-off frequency of the B-field measuring system. The electric field waveform includes the electrostatic field component owing to the intrinsic characteristic of the E-field measuring system.

In the results of the FFT, a DC component is in many cases generated by the computer in lower limit frequency $f_L = 1/T$, where T is the evaluated observation time. This DC com-

ponent is basically a square-wave pulse of the duration T, resulting in -20 dB/decade slope beginning at f_L. This part of the calculated Fourier spectrum does not correspond to reality[10].

Even if the waveforms of the electric field and magnetic flux density are very different, their FFT results are alike. In particular, the FFT result of the magnetic flux density is much same with in the oscillatory transient current. The difference between two resonance peaks at 390 kHz and 2 MHz for the magnetic flux density waveform is about 35 dB and is twice as much as that for the electric field waveform. This was originated because DC component of the electric field in the time domain is much more than that of the magnetic flux density.

Fig. 7 illustrates the magnetic flux density depending on the distance in parallel with the measuring point P in Fig. 3.

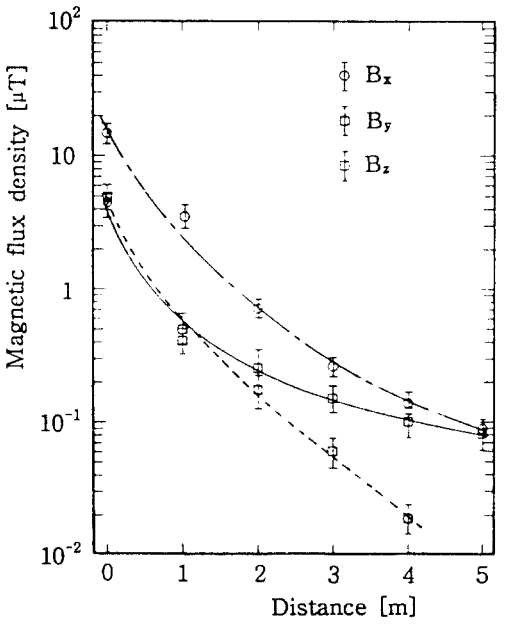

Fig. 7. Dependence of the magnetic flux density on the distance.

The dependence of the magnetic flux density B_z on the distance is similar to B_x. The data shows that the magnetic flux density is approximately reduced by a reciprocal of the square of the distance up to about 1.5 m thereafter reduced by a reciprocal of the distance. Also, the jitter of the magnetic flux density B_x is less than that of B_y and B_z.

3-2 Transient electric and magnetic fields in a high voltage laboratory

Fig. 8 shows a typical electric field waveform induced by a chopped impulse voltage and the FFT result at the measuring point A indicated in Fig. 4. The Marx generator, which is 8-stage charging type, has a considerable jitter during the triggering process.

The agitation at the front part of the chopped impulse voltage is due to a triggering sequence of the impulse voltage generator. The voltage applied to the spark gap G was about 320 kV. The electric field waveform is principally same as that as the chopped impulse voltage measured by means of the resistive divider. Since the chopped impulse waveform includes a large square-wave pulse, the higher frequency components are not obviously discreminated at the FFT result.

In order to analyze a valid Fourier spectrum, the signal in the time domain has to be measured with appropriate time bases. This work aimed at the evaluation of the time-changing electric and magnetic fields, which generally cause the severe electromagnetic interferences to the electronic circuits and

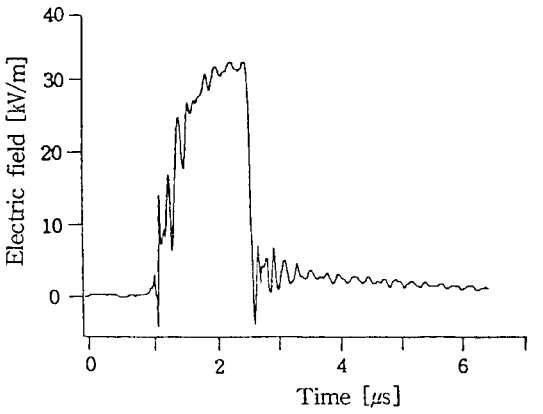

(a) Electric field waveform.

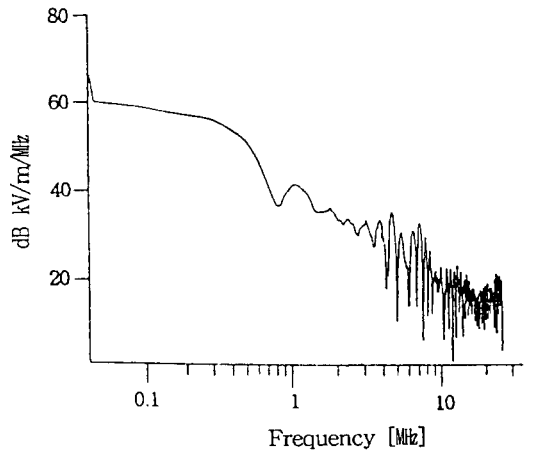

(b) FFT.

Fig. 8. The electric field waveform induced by a chopped impulse voltage at the measuring point A and its FFT.

control devices. In practice, it is comparatively easy to shield the low frequency electric field by using the thin aluminum foil and metallic cages. However the sufficient shielding of transient magnetic fields is very difficult unless the source is a low frequency magnetic fields.

Fig. 9 presents the magnetic flux density waveform induced by a chopped impulse voltage and the FFT results at the measuring point A. The first half of the waveform corresponds to the triggering sequence and characteristic of the Marx generator and the second half originates from the impulse chop-

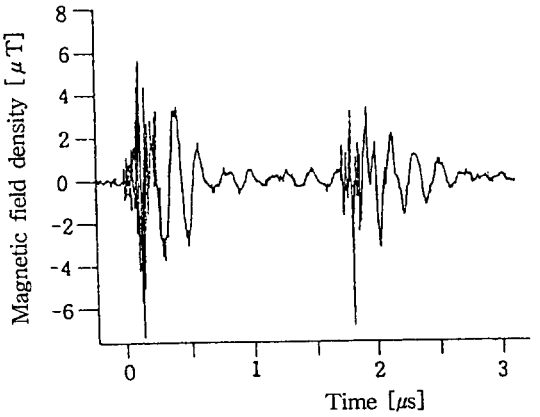

(a) Magnetic flux density waveform.

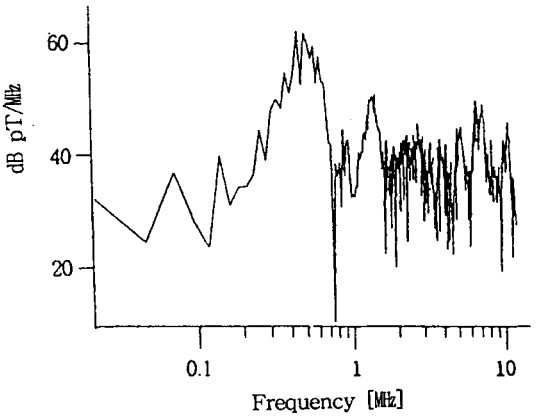

(b) FFT.

Fig. 9. Typical waveform of the magnetic flux density induced by a chopped impulse voltage at the measuring point A and its FFT.

ping of gap G.

The magnetic flux density waveform recorded after impulse chopping is similar to that before flashover of the spark gap G. The magnetic flux density waveform shows a damped oscillatory frequency of 500 kHz. The amplitude of the oscillatory frequency component of 500 kHz will be slightly underestimated by the limit of low cut-off frequency of the magnetic field measuring system. The FFT result indicates three resonance peaks at 0.5, 1.5 and 7 MHz, respectively.

Fig. 10(a) shows the electric field waveform and the FFT results measured at the measuring point B in Fig. 4. The initial part of the pulselike signal is to be shown the waveform after triggering radiation of impulse voltage generator. Fig. 10(b) shows the spectrum of the digitally recorded waveform in Fig. 10(a).

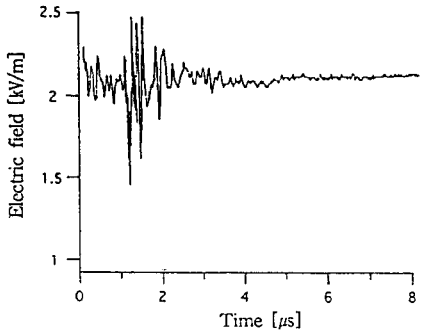

(a) Electric field waveform.

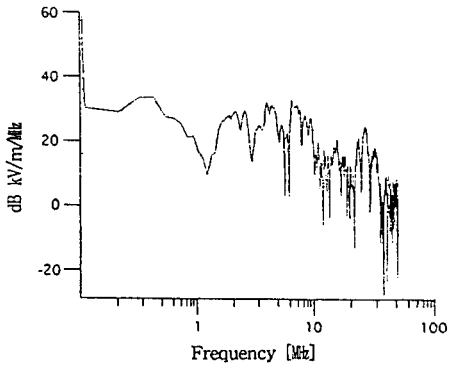

(b) FFT.

Fig. 10. The electric field waveform induced by a chopped impulse voltage at the measuring point B and its FFT.

Fig. 11 shows the magnetic flux density

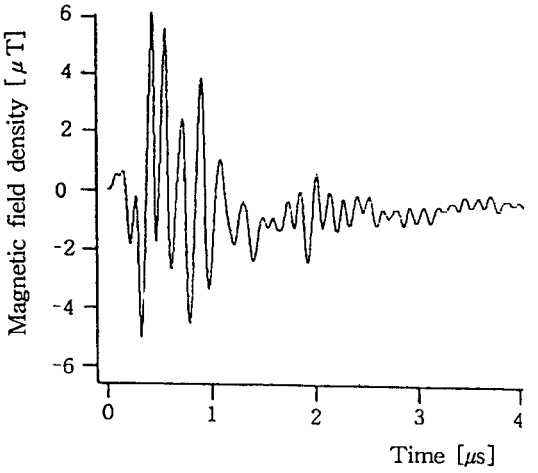

(a) Magnetic flux density waveform.

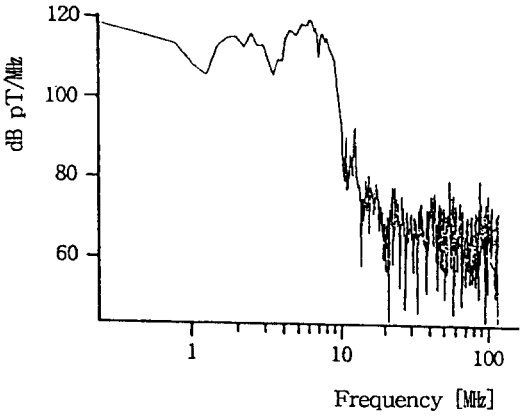

(b) FFT.

Fig. 11. The magnetic flux density waveform and the FFT results induced by a chopped impulse voltage at the measuring point C.

waveform and the FFT results measured at the measuring point C. But it is unsatisfactory that the transient electric field at the measuring point C was not detected by the E-field sensor used in this work because of the shielding effect of metallic fence.

The magnetic flux density at the outside of the metallic screen (point C) is on the whole lower than that at the inside of the metallic screen (point B) by about −10 dB pT/MHz. The significant variation for the essential characteristic of the magnetic flux density cannot be found. Furthermore, in the case of the outside of the metallic screen, no attenuation is seen within the frequency range up to 8 MHz and the average level is about 120 dB pT/MHz.

Ⅳ. Conclusions

The time-changing electric and magnetic fields were investigated by Marx generator with a chopping gap of the oscillatory transient current simulator, which simulate ground faults and/or short circuit currents of the real sized electric power equipments. The measured magnetic flux density waveform is approximately the same as the reference current waveform. The high frequency magnetic field is strongly caused by the gap discharge current at the beginning part owing to the Marx generator triggering sequence and is nearly identical with that after the chopped impulse. The obtained data and techniques, in this paper, are very useful in evaluating the electromagnetic shielding effectiveness and in predicting the electromagnetic compatibility (EMC) for equipments operated in extraneous electromagnetic field environments such as high voltage test, EMP and switching surges.

This work was supported by the Electrical Engineering & Science Research Center (Project No. 94-G-06) and the authors appreciate the financial support from the Korea Electric Power Corporation.

References

[1] R. Malewski, J. Huc and A. Podgoeski, "Electromagnetic Interference Field Induced by Discharges of HV Impulse Generators", *Proc. of 4th International Symposium on High Voltage Engineering(ISH)*, Paper no. 64, 10, 1983.

[2] Edmund K. Miller, "Time-Domain Measurements in Electromagnetics", *Van Nostrand Reinhold Company*, New York, pp. 175-210, 1986.

[3] K. Aria, et al, "Micro-Gap Discharge Phenomena and Television Interference", *IEEE Trans.*, vol. PAS-104, pp. 221-232, 1985.

[4] T. Kawamura, T. Nishimura, B. H. Lee and M. Ishii, "Generation Apparatus and Measuring System of Very Fast Transient Surges", *Proc. of Annual Conference of IEE of Japan*, Paper no. 1288, 1989.

[5] C. E. Baum, et al, "Sensor for Electromagnetic Pulse Measurement Both Inside and Away from Nuclear Source Regions", *IEEE Trans.*, vol. AP-26, pp. 22-35, 1978.

[6] F. E. Terman and J. M. Petit, "Electronic Measurements", Mcgraw-Hill Book

Co., INC., pp. 122-128, 1952.

[7] B. H. Lee, et al, "Transient Electric Field Analysis with a New Measuring System around High Voltage Apparatus", *KIEE Trans.*, vol. 46, no. 1, pp. 133-141, 1997.

[8] J. A. Cameron, "Self-Integrating Magnetic Field Sensors", *IEEE Trans.*, CH-2116-2, pp. 98-105, 1985.

[9] IEEE Standards Board, "IEEE Standard Procedures for Measurement of Power Frequency Electric and Magnetic Fields from AC Power Lines ; ANSI /IEEE Std.-644", pp. 17-21, 1987.

[10] A. Aron, L. Fickert, F. Reisinger and W. Wais, "Fourier Spectrum as a means of Representation and Evaluation of Transient Voltage Surges in GIS", *Proc. of 5th ISH*, Paper 12.04, 1987.

이 복 희

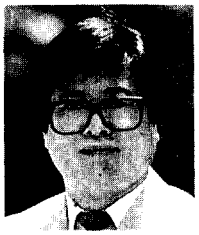

1954년 6월 29일생

1980년 2월 : 인하대학교 공과대학 전기공학과(공학사)

1987년 2월 : 동 대학원 전기공학과 (공학박사)

1988년 4월~1989년 9월 : 일본 동경대 생산기술연구소 객원연구원

1990년 3월~현재 : 인하대학교 공과대학 전기공학과 부교수

[주 관심분야] EMI /EMC, 전자계 측정 및 해석, 뇌방전 현상, 고전압 및 기체절연재료 분야

안 창 환

1959년 11월 4일생

1983년 2월 : 원광대학교 공과대학 전기공학과(공학사)

1991년 2월 : 인하대학교 대학원 전기공학과(공학석사)

1995년 3월~현재 : 동대학원 전기공학과 박사과정

[주 관심분야] EMI /EMC, 뇌방전 현상, 전력계통운용, 고전압현상론, 뇌서지보호, GIS 성능해석

이 경 옥

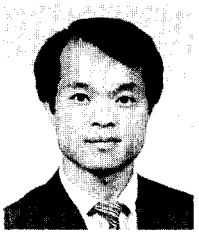

1960년 6월 24일생

1987년 2월 : 인하대학교 공과대학 전기공학과(공학사)

1989년 2월 : 동 대학원 전기공학과(공학석사)

1988년 12월~1991년 2월 : 동양나이론 해외사업부 Royal Project팀 사원

1996년 3월~현재 : 동 대학원 전기공학과 박사과정

[주 관심분야] EMI /EMC, 전자계 센서, 기체절연재료 특성분석, 뇌서지 보호장치 개발